

# Experimental Proof of Adjustable Single-Knob Ion Beam Emittance Partitioning

L. Groening,<sup>\*</sup> M. Maier, C. Xiao, L. Dahl, P. Gerhard, O. K. Kester, S. Mickat, H. Vormann, and M. Vossberg  
*GSI Helmholtzzentrum für Schwerionenforschung GmbH, Darmstadt D-64291, Germany*

M. Chung

*Ulsan National Institute of Science and Technology, Ulsan 698-798, Republic of Korea*

(Received 26 September 2014; published 30 December 2014)

The performance of accelerators profits from phase-space tailoring by coupling of degrees of freedom. Previously applied techniques swap the emittances among the three degrees but the set of available emittances is fixed. In contrast to these emittance exchange scenarios, the emittance transfer scenario presented here allows for arbitrarily changing the set of emittances as long as the product of the emittances is preserved. This Letter is the first experimental demonstration of transverse emittance transfer along an ion beam line. The amount of transfer is chosen by setting just one single magnetic field value. The envelope functions (beta) and slopes (alpha) of the finally uncorrelated and repartitioned beam at the exit of the transfer line do not depend on the amount of transfer.

DOI: 10.1103/PhysRevLett.113.264802

PACS numbers: 41.75.Ak, 41.85.Ct, 41.85.Ja, 41.85.Lc

Important figures of merit for any accelerator are the beam emittances it provides at its exit. Emittances are measures for the amount of phase space being occupied by the particle distribution. Along an ideal linear focusing lattice the dynamics in the three phase-space planes, which we refer to as “planes” in the following, are not coupled and the emittances remain constant in each plane. Unavoidable coupling from fringe fields or from dispersion increases the emittances in the coupled planes. Accordingly, lattice elements were designed in order to minimize the coupling, except for dedicated applications such as spectrometers, for instance. However, the case may arise where the performance of an accelerator is well within the emittance budget in one plane but far beyond it in another one. Exchange of emittances between two planes may be sufficient to remain within all emittance budgets. Such schemes must involve interplane coupling.

Exchange of the two transverse emittances by a quadrupole triplet rotated by 45° (skew triplet) is state of the art. Brinkmann *et al.* [1] proposed creation of beams with strongly different transverse emittances, i.e., round-to-flat adapters, and Refs. [2–4] report on the successful conduction of the experiment. They used the solenoidal field of the electron source as an interplane coupling element as well as a subsequent skew triplet. Application of this concept to ion beams is proposed in Refs. [5–7]. Exchange between the longitudinal and one transverse plane was considered and/or demonstrated in Refs. [8–10]. Coupling was provided through installation of a transversely deflecting cavity inside a dispersive section created by bending magnets. Several studies were done aiming at finding the best-suited coupling scenarios to optimize the emittance exchange [11] or to combine it with strong bunch length compression [12]. A recent review of longitudinal to

transverse emittance exchange beam lines can be found in Ref. [13].

A common property of all emittance shaping beam lines operated so far is that neither the set of values of the final emittances has been changed nor has changing of this set been foreseen in the designs of the beam lines. Exchange beam lines just reassign the emittance values to the planes. Final emittances of round-to-flat adapters are given by the field strength of the solenoid at the source. The set of final emittances achieved by these beam lines is called the set of eigenemittances [14]. The beam lines applied so far preserve the set of eigenemittances and the product of the  $n$  eigenemittances is equal to the  $2n$ -dimensional root-mean-squared (rms) emittance of the beam. In the following, we refer to two-dimensional geometric rms emittances defined as

$$\epsilon_u := \sqrt{\langle u^2 \rangle \langle u'^2 \rangle - \langle uu' \rangle^2}, \quad (1)$$

where  $u$  is the particle coordinate and  $u'$  is its derivative with respect to the longitudinal coordinate. The beta function and the alpha parameter are defined as

$$\beta_u := \frac{\langle u^2 \rangle}{\epsilon_u}, \quad \alpha_u := -\frac{\langle uu' \rangle}{\epsilon_u}. \quad (2)$$

Transverse emittance transfer as proposed in Refs. [7,15] instead offers a tool to arbitrarily choose the final emittances as long as their product is kept constant. It changes the set of eigenemittances. The beam line is sketched in Fig. 1. Two quadrupole magnet doublets focus the beam to a solenoid. A stripping foil is installed in the center of the solenoid. Increasing the ion beam charge state by passing

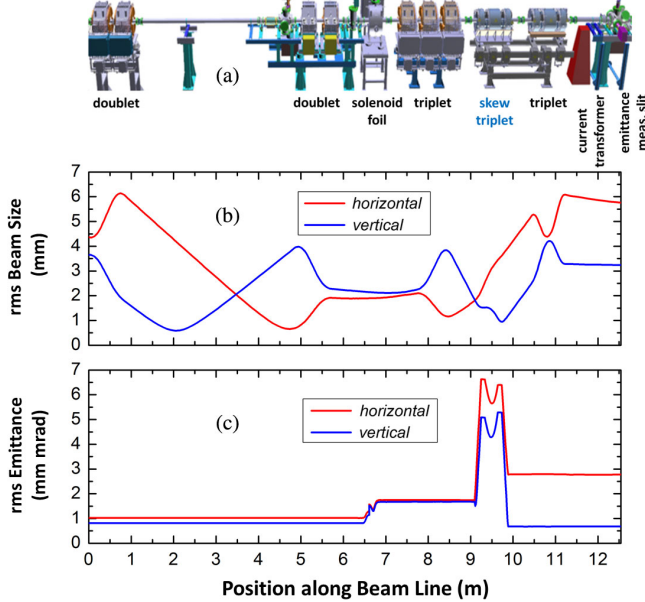


FIG. 1 (color online). Beam line of EMTEX (Emittance Transfer Experiment) (a), vertical (blue) and horizontal (red) rms beam sizes (b), and rms beam emittances (c) along the beam line for a solenoid field of 0.9 T (see text).

the beam through a stripping medium is state of the art in ion accelerators; see Ref. [16], for instance. The outer electrons of the incoming ions are removed and the ions experience stochastic angular scattering and energy straggling. As a net effect, the charge state is increased and the angular distribution is broadened as well as the beam energy spectrum. However, for intermediate to heavy mass ions, charge state stripping is mandatory in order to perform acceleration at reasonable efficiency. Change of charge state in the solenoid changes the set of eigenemittances. The field strength of the solenoid determines the amount of transfer between the eigenemittances. It is followed by a quadrupole triplet and a skewed quadrupole triplet. The latter preserves the eigenemittances but serves to remove interplane correlations introduced by the solenoid. It is followed by a regular quadrupole triplet to rematch the beam for the subsequent transport. Finally, a slit-grid beam emittance meter allows for measuring the phase-space distribution in the horizontal and vertical planes. The slit determines the position of the phase-space element. A subsequent grid measures the angular distribution of the ions that passed the slit. By moving the slit and recording the angular distribution at each slit position, the full phase-space distribution is recorded. A detailed description of the concept of EMTEX (Emittance Transfer Experiment) and the beam line itself is given in Refs. [7,15,17].

EMTEX has two very convenient features. The setting of the beam line behind the solenoid does not depend on the solenoid field strength  $B$ . The setting provides excellent decoupling if it is determined for a solenoid field  $B_0$  and if the applied field  $B$  satisfies  $|B| \leq |B_0|$ . Additionally, the

Twiss parameters  $\beta$  and  $\alpha$  provided at its exit do not change with the field strength  $B$ . These very comfortable decoupling and rematching features were observed in simulations [15] and were analytically explained later [18]. Hence EMTEX is a one-knob tool for transverse emittance partitioning. The knob is the solenoid field strength  $B$ .

EMTEX was installed [19] in 2013 along the transfer channel from GSI's Universal Linear Accelerator (UNILAC) [20] to the synchrotron. For the experiment, a low-intensity (i.e., negligible space charge effects) beam of  $^{14}\text{N}^{3+}$  at 11.4 MeV/u was used. The relative momentum spread of the beam was less than  $10^{-3}$ . First, all EMTEX magnets were turned off and the stripping foil was removed from the solenoid. Full beam transmission was assured by using beam current transformers installed in front of and behind EMTEX. In order to assure that the beam in front of EMTEX does not exhibit already relevant interplane correlations, the  $(x, y)$  beam distribution was observed on a fluorescent screen for different settings of a quadrupole magnet being installed in front of the screen. The absence of correlation in  $(x, y)$  implied insignificant residual correlations between the two planes.

In the following step, beam emittances were measured in both planes at the exit of EMTEX. The obtained Twiss parameters together with the settings of the first two doublets were used to determine the beam Twiss parameters at the entrance to the first doublet of EMTEX. A horizontal (vertical) rms emittance of 1.04 (0.82) mm mrad was measured. Both doublets were set to provide a small beam with double waist at the location of the stripping foil. The foil (carbon,  $200 \mu\text{g}/\text{cm}^2$ , 30 mm in diameter) was moved into the solenoid. The measured beam current transmission through the complete EMTEX beam line increased by a factor of  $2.3 = 7/3$  as expected from increase of the ion charge state by stripping of the beam from  $3+$  to  $7+$ . Beam phase probes behind EMTEX were used to detect eventual beam energy loss induced by the foil. Within the resolution of the phase probes, we assume that the mean energy loss is close to the calculated value of 0.026 MeV/u from the ATIMA code and that the amount of energy straggling can be neglected. The same code was used to calculate the increase of the square of the rms beam divergence by  $(0.474 \text{ mrad})^2$  per transverse plane. After determining all required input parameters, the solenoid field was set to 0.9 T. Applying a numerical routine, the three triplets behind the solenoid were set to decouple the beam and to provide for a beam with small vertical and large horizontal emittance together with full transmission through the entire setup. These gradients were set and full beam transmission was preserved. Just slight adjustment of the beam center using dipole-corrector magnets was needed to recenter the beam in the emittance meter. This was required due to residual misalignment of the solenoid axis with respect to the beam axis. For the setting mentioned above, both transverse rms emittances were measured.

Afterwards the solenoid field was reduced stepwise to 0 T. The solenoid field  $B_i$  was set by following the remanence-mitigating path  $B_{i-1} \rightarrow B_{\max} \rightarrow 0T \rightarrow B_i$ . All quadrupole magnet gradients were kept constant. For each solenoid setting, full transmission was preserved and both emittances were measured. The upper part of Fig. 2 plots the measured rms emittances behind EMTEX as functions of the solenoid field strength. With increasing solenoid field, the vertical emittance decreases while the horizontal increases. The product of the two emittances remains constant within the precision of the measurement. This behavior is in full agreement with theoretical predictions from Ref. [15] and

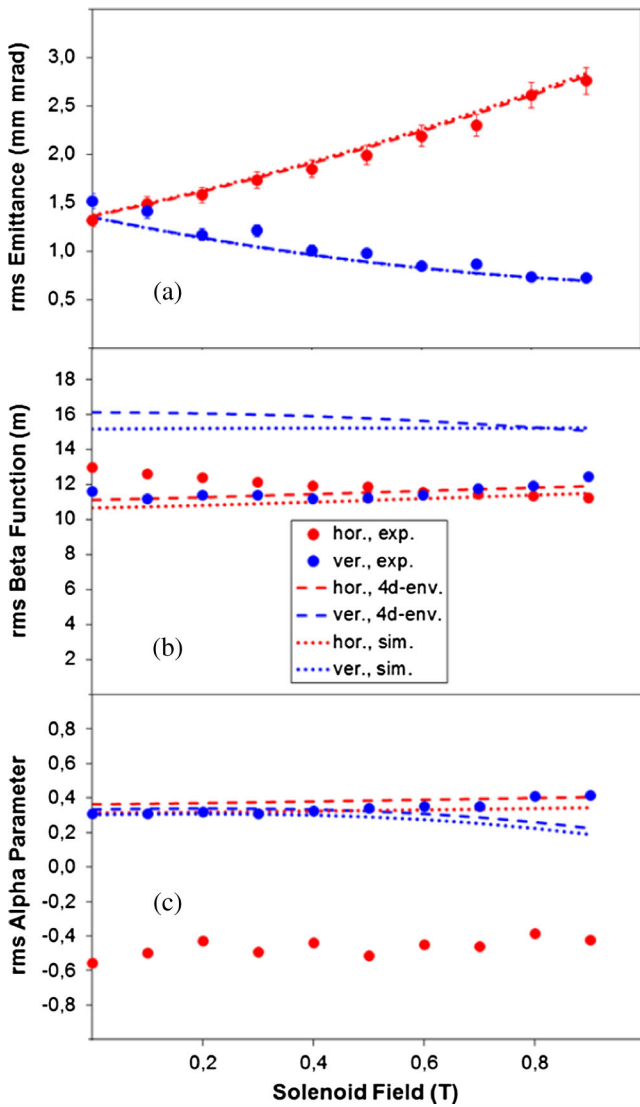


FIG. 2 (color online). Vertical (blue) and horizontal (red) rms emittances (a), beta functions (b), and alpha parameters (c) at the exit of the EMTEX beam line as functions of the solenoid field strength. All other settings were kept constant. Shown are results from measurements (dots), from application of the 4d-envelope model for coupled lattices (dashed lines), and from tracking simulations (dotted lines).

with tracking simulations with TRACK [21] using magnetic field maps. It is also in agreement with calculations that apply the recently developed 4d-envelope model for coupled lattices [22–25]. The observed emittance separation under variation of the solenoid field only confirms that EMTEX is a one-knob tool for adjustable emittance partitioning. Beam envelopes and emittances along the beam line for a solenoid field of 0.9 T as obtained from tracking simulations are plotted in Fig. 1.

Figure 3 displays measured phase-space distributions as functions of the solenoid field strength. It demonstrates that the shapes of the occupied areas in phase space and especially the shapes of the corresponding  $4 \times$  rms ellipses almost do not depend on the solenoid field strength. The corresponding parameters  $\beta$  and  $\alpha$  are plotted in Fig. 2. Although there are small discrepancies between theory and measurements for  $\beta_y$  and  $\alpha_x$ , the experimental results are in full agreement with the observation from simulations reported in Ref. [15] and with the properties of EMTEX derived analytically [18]. These references assumed a beam with exactly equal transverse emittances at the entrance of EMTEX. The beam emittances in the experiment differed by 23% from each other. However, the quasi-invariance of the final ellipse shapes is in excellent agreement with the 4d-envelope model and with tracking simulations also for the present experiment. Accordingly, the experimental data also confirm that EMTEX is a one-knob emittance partitioning tool that preserves the beam envelope functions  $\beta$  and  $\alpha$  at its exit, if the initial beam emittances are similar. This feature makes it obsolete to rematch the envelopes as a function of the desired emittance partitioning once the partitioning is completed.

As the amount of emittance partitioning is given by the solenoid field strength [15], inversion of the solenoid field swaps the behaviors of the measured emittances displayed in Fig. 2; i.e., for negative solenoid field strengths the vertical emittance increases and the horizontal one decreases with the field strength. This could not be tested experimentally, since the solenoid power converter was unipolar. Inversion of the solenoid field strength is fully equivalent to inversion of the skew quadrupole magnet

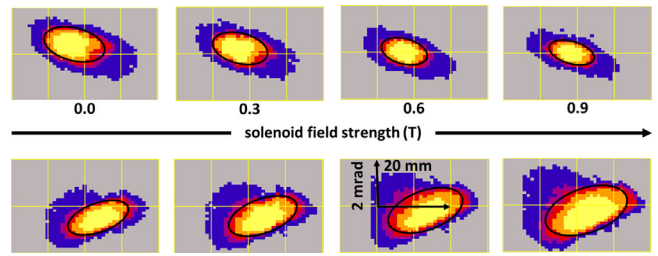


FIG. 3 (color online). Vertical (upper) and horizontal (lower) phase-space distributions measured at the exit of the EMTEX beam line as functions of the solenoid field strength. All other settings were kept constant. Black ellipses indicate the  $4 \times$  rms ellipses.

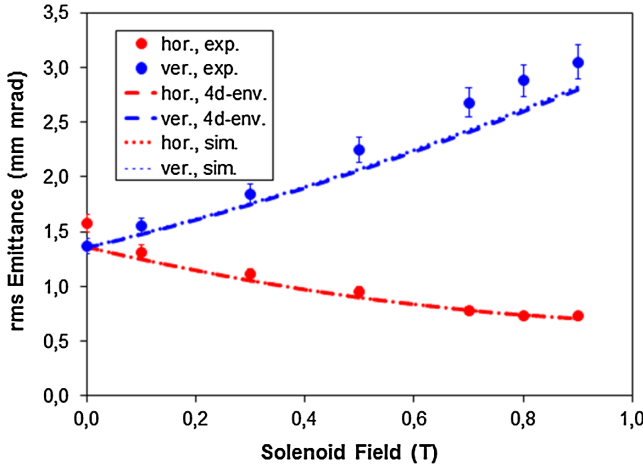


FIG. 4 (color online). Vertical (blue) and horizontal (red) rms emittances at the exit of the EMTEX beam line as functions of the solenoid field strength. All other settings were kept constant. Shown are results from measurements (dots), from application of the 4d-envelope model for coupled lattices (dashed line), and from tracking simulations (dotted line). With respect to Fig. 2, the gradients of the skew quadrupole triplet are inverted.

gradients, while keeping all other gradients and the solenoid field constant. Inversion of the skew gradients corresponds to rotation of the skew quadrupole magnets by  $90^\circ$ , i.e., to swapping the transverse planes. Accordingly, the ratio of emittance partitioning is inverted for inverted skew quadrupole triplet gradients. This was verified experimentally as shown in Fig. 4. Also for inverted skew quadrupole magnet gradients, preservation of the orientations and shapes of the measured phase-space distributions was observed. Just the sizes of the corresponding  $4 \times$  rms ellipses changed with the solenoid field strength. For inverted polarity of the skew quadrupole triplet, the agreement with theory and with simulations is still good but slightly worse than for the case shown in Fig. 2. Additionally, for a given solenoid field value, the horizontal emittance values shown in Fig. 4 are not exactly equal to the vertical emittance values shown in Fig. 2. According to theory they should be equal. However, the differences are very small. We attribute them to remanence effects in the solenoid and in the bipolar skew triplets.

This work was partly supported by the 2014 Research Fund (1.140075.01) of UNIST (Ulsan National Institute of Science and Technology).

\*la.groening@gsi.de

- [1] R. Brinkmann, Y. Derbenev, and K. Flöttmann, DESY Report No. TESLA-99-09, 1999.
- [2] D. Edwards, H. Edwards, N. Holtkamp, S. Nagaitsev, J. Santucci, R. Brinkmann, K. Desler, K. Flöttmann, I. Bohnet, and M. Ferrario, in *Proceedings of the XX Linear Accelerator Conference, Monterey, CA, 2000*, edited by A. Chao, eConf e000842 (2000), p. 112.
- [3] R. Brinkmann, Y. Derbenev, and K. Flöttmann, *Phys. Rev. ST Accel. Beams* **4**, 053501 (2001).
- [4] P. Piot, Y.-E. Sun, and K.-J. Kim, *Phys. Rev. ST Accel. Beams* **9**, 031001 (2006).
- [5] P. Bertrand, J. P. Biarrotte, and D. Uriot, in *Proceedings of the 10th European Accelerator Conference, Edinburgh, Scotland, 2006*, edited by J. Poole and C. Petit-Jean-Genaz (Institute of Physics, Edinburgh, Scotland, 2006).
- [6] C. Xiao, L. Groening, and O. K. Kester, *Nucl. Instrum. Methods Phys. Res., Sect. A* **738**, 167 (2014).
- [7] L. Groening, *Phys. Rev. ST Accel. Beams* **14**, 064201 (2011).
- [8] P. Emma, Z. Huang, K.-J. Kim, and P. Piot, *Phys. Rev. ST Accel. Beams* **9**, 100702 (2006).
- [9] Y.-E. Sun, P. Piot, A. Johnson, A. H. Lumpkin, T. J. Maxwell, J. Ruan, and R. Thurman-Keup, *Phys. Rev. Lett.* **105**, 234801 (2010).
- [10] D. Xiang and A. Chao, *Phys. Rev. ST Accel. Beams* **14**, 114001 (2011).
- [11] B. E. Carlsten, K. A. Bishopberger, L. D. Duffy, S. J. Russell, R. D. Ryne, N. A. Yampolsky, and A. J. Dragt, *Phys. Rev. ST Accel. Beams* **14**, 050706 (2011).
- [12] B. E. Carlsten, K. A. Bishopberger, S. J. Russell, and N. A. Yampolsky, *Phys. Rev. ST Accel. Beams* **14**, 084403 (2011).
- [13] J. Thangaraj, in *Proceedings of the XXVII Linear Accelerator Conference, Geneva, Switzerland, 2014*, edited by C. Carli (CERN, Geneva, Switzerland, 2014).
- [14] A. J. Dragt, F. Neri, G. Rangarajan, , *Phys. Rev. A* **45**, 2572 (1992).
- [15] C. Xiao, O. K. Kester, L. Groening, H. Leibrock, M. Maier, and M. Rottländer, *Phys. Rev. ST Accel. Beams* **16**, 044201 (2013).
- [16] H. Okuno, N. Fukunishi, A. Goto, H. Hasabe, H. Imao, O. Kamigaito, M. Kase, H. Kuboki, Y. Yano, and S. Yokouchi,, *Phys. Rev. ST Accel. Beams* **14**, 033503 (2011).
- [17] C. Xiao, L. Groening, and O. Kester, in *Proceedings of the 52nd ICFA Advanced Beam Dynamics Workshop, Beijing, China, 2012*, edited by J. Wang (Institute of High Energy Physics, Beijing, China, 2012).
- [18] L. Groening, arXiv:1403.6962.
- [19] M. Maier, L. Groening, C. Mühlé, I. Pschorn, P. Rottländer, C. Will, C. Xiao, and M. Chung, in *Proceedings of the 5th International Particle Accelerator Conference, Dresden, Germany, 2014*, edited by C. Petit-Jean-Genaz (CERN, Geneva, Switzerland, 2014).
- [20] W. Barth, L. Dahl, L. Groening, J. Glatz, S. Richter, and S. Yaramyshev, in *Proceedings of the XXII Linac Conference, Lübeck, Germany, 2004*, edited by V. R. W. Schaa (DESY, Hamburg, Germany, 2004).
- [21] P. Ostroumov, “TRACK version 37 User Manual,” <http://www.phy.anl.gov/atlas/TRACK/>.
- [22] H. Qin, M. Chung, and R. C. Davidson, *Phys. Rev. Lett.* **103**, 224802 (2009).
- [23] H. Qin, R. C. Davidson, M. Chung, and J. W. Burby, *Phys. Rev. Lett.* **111**, 104801 (2013).
- [24] H. Qin, R. C. Davidson, J. W. Burby, and M. Chung, *Phys. Rev. ST Accel. Beams* **17**, 044001 (2014).
- [25] M. Chung, H. Qin, L. Groening, R. C. Davidson, and C. Xiao, *Phys. Plasmas* (to be published).